

Effect of Au coating on the magnetic and structural properties of Fe nanoclusters for use in biomedical applications: A density-functional theory study

Q. Sun,^{1,2,*} A. K. Kandalam,² Q. Wang,² P. Jena,² Y. Kawazoe,³ and M. Marquez¹

¹*Interdisciplinary Network of Emerging Science and Technologies (I'NEST Group), PMUSA, Richmond, Virginia 23234, USA*

²*Physics Department, Virginia Commonwealth University, Richmond, Virginia 23284, USA*

³*Institute for Material Research, Tohoku University, Sendai 980-8577, Japan*

(Received 25 January 2006; published 7 April 2006)

In this paper, we report the first systematic theoretical study of gold-coated iron nanoclusters, aiming at understanding the magnetic properties of this core-shell structure used in biomedical applications. The calculations based on density-functional theory focus on the effect of gold coating on the magnetic and structural properties of iron clusters of various sizes, and the reaction of the bare and coated iron clusters with oxygen. Our results show that the magnetic moment of iron nanocluster with gold coating is still significantly higher than that in bulk Fe; the coupling between Fe atoms remained ferromagnetic and is insensitive to the thickness of the Au coating. Furthermore, oxygen remains molecular on a gold-coated Fe nanoparticle while it dissociates on a bare Fe nanoparticle. The improved chemical stability by gold coating prevents the iron core from oxidation as well as the coalescence and formation of thromboses in the body. Thus it is shown that gold coating is very promising for the magnetic particles to be functionalized for targeted drug delivery.

DOI: [10.1103/PhysRevB.73.134409](https://doi.org/10.1103/PhysRevB.73.134409)

PACS number(s): 75.75.+a, 73.22.-f, 31.15.Ar, 71.15.Nc

I. INTRODUCTION

Conventional methods of treating malignant tumors such as surgery, radiation, and/or chemotherapy are either invasive or have adverse side effects. A desired goal in cancer therapy for many years has been to find ways by which cancer cells can be selectively destroyed without damaging normal cells. Nanostructured particles which have the same length scales as those of tumors provide some attractive possibilities where this noble goal may some day be achieved. In particular, the magnetically directed drug delivery combined with hyperthermia can greatly improve the performance of current procedures. The strategy is to implant a nanoparticle near a cancer cell that can be heated through near infrared (NIR) light or an alternating magnetic field. The resulting heat can then destroy the tumor cells without damaging the healthy tissues. Since the magnetic field can penetrate deep into the tissue, the use of magnetic fluid hyperthermia provides a versatile method to treat a variety of tumors such as anaplastic astrocytomas or glioblastomas. An ideal nanoparticle for this application should be a strong magnet, biocompatible, and resistant to corrosion as well as aggregation.

The conventional magnetic nanoparticles that are widely used in experiments and animal testing involve iron oxides. However, the magnetic strength of iron oxides is not as high as that of pure iron and there is significant interest in developing alternative high moment nanoparticles for specific biomedical applications. In fact, the ability to control size, shape, and composition of magnetic iron nanoparticles can provide flexibility for applications in cell labeling, magnetic resonance imaging (MRI), drug delivery, and DNA separation.¹⁻³ Unfortunately, bare Fe particles cannot directly be used for the following reasons: (1) Free iron is toxic because of its propensity to induce the formation of dangerous free radicals. (2) They can easily aggregate to form larger particles, thus resulting in the formation of thromboses. (3)

They can easily be oxidized, which in turn will weaken their magnetic property. In order to circumvent the above problems, Fe nanoparticles need to be coated so that they retain their high magnetic moment, and remain nontoxic, biocompatible, and chemically stable.

Gold has been recognized as the best candidate for coating due to its bio-compatibility, functionality with various enzymes, chemical inertness, and flexible geometries such as rings, cages, and tubes.⁴⁻⁹ Recently, the synthesis and characterization of gold-coated iron nanoparticles and the study of their magnetic properties have become the focus of many experimental studies.^{10,11} Using microemulsion or reverse micelle method,¹² Lin *et al.* were successful in synthesizing gold-coated iron nanoparticles where the peaks corresponding to iron oxide nanoparticles were not seen in the x-ray diffraction (XRD) analysis. This indicates that the gold coating on the iron nanoparticles is protecting them rather well from oxidation. Cho and co-workers reported the synthesis of iron-gold core-shell nanoparticles with large iron cores that exhibit ferromagnetism at room temperature.¹³ In another experimental study,¹⁴ gold-coated acicular and spherical shaped iron nanoparticles were prepared and their morphology and magnetic properties were characterized using transmission electron microscopy (TEM) and alternate gradient magnetometry. It has been found that the gold-coated nanoparticles were more resistant to oxidation and corrosion than the uncoated particles, and the gold shell was more uniformly distributed on the spherical particles than on the acicular ones.

In spite of these experimental studies, a fundamental understanding of how gold interacts with an iron core is still lacking. For example: (1) Does gold coating enhance or reduce the magnetic moment of iron and how does it change as the thickness of the coating is increased? (2) Do the iron atoms continue to couple ferromagnetically? (3) Does the geometry of iron core change when it is coated with gold?

(4) How does the reactivity of Fe clusters toward oxygen change with Au coating? No experiments to our knowledge have measured the magnetic moment of a Fe core coated with gold. On the theoretical front, very few studies have been carried out on noble metal coated metal nanoparticles. Tight binding based theoretical calculations¹⁵ were performed to understand the properties of Cu covered cobalt and Ag covered cobalt clusters. In a density-functional theory based study,¹⁶ the different magnetic properties between palladium coated and alloyed nickel clusters were investigated. As to our knowledge, there are no theoretical studies of gold-coated iron clusters. Motivated by the imbalance between the experiments and theoretical studies of the gold-coated iron clusters, and the lack of fundamental understanding of the shell-core interactions, we have initiated a theoretical study of gold-coated iron nanoclusters.

In this paper, we report the results of the first systematic theoretical investigation of the structural and magnetic properties of gold-coated iron nanoclusters at various size ranges and provide answers to the aforementioned important questions on the shell-core interactions. We show that the coating of gold not only prevents the iron core from oxidation but also keeps the strong magnetic nature of iron alive. Our theoretical work not only complements the oxidative properties of gold-coated Fe nanoparticles but also shows further that the magnetic moment of the iron core is larger than its bulk value. These studies provide some insight for gold-coated Fe nanoparticles in biomedical applications.

II. COMPUTATIONAL METHODS

The focus of this study was to study the magnetic property of Fe nanoparticles and how they are affected by gold coating and reaction with oxygen. Since the origin of magnetism quantum mechanical phenomenon, we used density-functional theory (DFT). The ground state geometries of $\text{Fe}_2\text{-Au}_n$ ($n=1-6$, and 18) clusters were obtained using GAUSSIAN03 program suite.¹⁷ The “frozen core” Lanl2dz basis set for Au and 6-311G* basis set for Fe were employed in the calculations. The geometrical parameters of $\text{Fe}_2\text{-Au}_n$ clusters were completely optimized, without any symmetry constraints and for all the possible spin configurations. The convergence criteria for the gradient force and the energy were set to 10^{-4} Hartree/Å and 10^{-9} Hartree, respectively. For the larger systems (Fe_xAu_y , $x=1, 13$, $y=12, 42, 54, 134$; $\text{Fe}_{13}\text{Au}_{42}\text{-O}_2$), however, GAUSSIAN03 calculations are computationally prohibitive. For these studies, we used a plane-wave basis set with the projector augmented plane-wave (PAW) method as implemented in the Vienna *ab initio* Simulation Package (VASP).¹⁸ We have used supercells with 15 Å vacuum spaces along x , y , and z directions for all the calculated structures. The Γ point is used to represent the Brillouin zone due to the large supercell. The energy cutoff was set to 400 eV and the convergence in energy and force were 10^{-4} eV and 1×10^{-3} eV/Å, respectively. The generalized gradient approximation (GGA) to DFT was used in all these calculations. The gradient corrected exchange functional due to Becke,¹⁹ combined with gradient corrected Perdew-Wang²⁰ correlation functional (BPW91) were used.

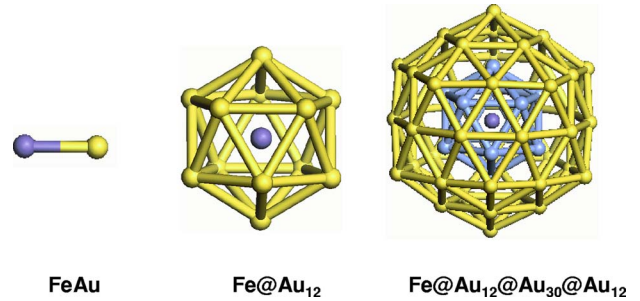


FIG. 1. (Color online) Geometries of Fe atom wrapped in gold.

The accuracy of our numerical procedure was well tested in our previous studies.^{7,21-23}

III. RESULTS

A. Magnetic moment of Fe_1Au_n ($n=1, 12$, and 54) clusters

Our first objective is to calculate the magnetic moment of a Fe atom interacting with Au atoms by coating a Fe atom with successive shells of Au atoms. We start with a Fe atom first interacting with a single Au atom and then embedding the Fe atom inside Au icosahedra containing 12 and 54 atoms. These clusters are labeled as Fe_1Au_1 , $\text{Fe}_1 @ \text{Au}_{12}$, and $\text{Fe}_1 @ \text{Au}_{12} @ \text{Au}_{30} @ \text{Au}_{12}$. Figure 1 shows the equilibrium geometries of these complexes while their structural parameters and magnetic moments are listed in Table I. Here, the magnetic moment is obtained using Wigner-Seitz cell partition method while the total magnetic moment includes the contributions from Fe core and Au shell. For an isolated Fe atom, the magnetic moment is $4 \mu_B$ based on the Hund's rule. When one Au atom is attached to a Fe atom, a FeAu dimer is formed with a bond length of 2.330 Å. Due to the hybridization between Au 6s and Fe 3d orbitals, the magnetic moment of Fe is reduced to $3.442 \mu_B$, and the Au atom is polarized ferromagnetically with a moment of $0.197 \mu_B$. In $\text{Fe} @ \text{Au}_{12}$ cluster the Fe atom is fully wrapped in an icosahedral shell. The distance between the Fe atom and the gold shell has increased to 2.713 Å. The magnetic moment of the Fe atom is reduced to $3.0 \mu_B$ and is antiferromagnetically coupled to the Au atoms, each of which carries a moment of $-0.057 \mu_B$. Although the larger distance between Fe and Au atoms would cause the Fe moment to increase, the net reduction in the Fe moment is a result of hybridization of Fe 3d orbitals with 6s orbitals of the 12 Au atoms.

To see if the moment on Fe will further reduce with the thickness of the gold shell, we added 42 more Au atoms to $\text{Fe} @ \text{Au}_{12}$ thus forming $\text{Fe}_1 @ \text{Au}_{12} @ \text{Au}_{30} @ \text{Au}_{12}$ cluster. In this case, the Fe atom is wrapped with two complete icosahedral shells. The distance between Fe atom and the first Au shell is 2.718 Å, the Au-Au bond lengths in the first and second shell are 2.864 and 2.875 Å, respectively. The distance between these two Au shells is 2.741 Å. The magnetic moment of the Fe atom is still $3.0 \mu_B$; whereas, the induced moment on Au atoms is totally changed. In the first shell, all the 12 Au atoms are equivalent with the moment of $0.034 \mu_B$. In the second shell, there are two unequivalent Au

TABLE I. Bond length R (Å) and magnetic moment μ (μ_B) for Fe atom wrapped with gold.

	Fe ₁	Fe ₁ Au ₁	Fe ₁ @Au ₁₂	Fe ₁ @Au ₁₂ @Au ₃₀ @Au ₁₂	Comparison
μ_{Fe}	4.0	3.442	3.00	3.0	3.05 (Fe impurity in Au bulk) ^a 2.95 (Fe-Au alloy) ^a 2.84 (Fe-Au overlayer) ^b 2.80 (Fe-Au multilayer) ^c
μ_{Au}		0.197	-0.057	0.034 (1st shell) 0.012 (2nd shell) 0.005 (3rd shell)	<0.07 (overlayer) ^d 0.036-1.105 (multilayers) ^c
R_{Fe-Au}		2.330	2.713	2.718	
R_{Au-Au}			2.852	2.684 (1st shell) 2.875 (2nd shell) 2.741 (1st, 2nd shell)	

^aReference 24.^bReference 25.^cReference 26.^dReference 22.

atoms (30+12) with the moment of 0.012 and 0.005 μ_B . It is interesting to note that the moment of a Fe impurity in bulk Au is found to be 3.05 μ_B ,²⁴ while the moment of Fe is Fe-Au alloy is 2.95 μ_B .²⁴ In the overlayer and multilayers, the Fe moment is about 2.8 μ_B and the induced Au moment is about 0.036~0.105 μ_B .^{25,26} Thus, one could conclude that the magnetic moment of a Fe atom in Au has saturated to a value of about 3.0 μ_B . This is particularly important since the magnetic moment of Fe in the bulk is only 2.2 μ_B .

B. Magnetic coupling between Fe atoms in Fe₂Au_{*n*} (*n*=1-6,18), clusters

Once it is established that the magnetic moment of the Fe atom interacting with Au is even higher than that in the bulk Fe, it is important to examine if the interaction between the Fe atoms remains ferromagnetic. We study this by sequential addition of Au atoms to a Fe₂ dimer. In Fig. 2, we show the ground state geometries for Fe₂Au_{*n*} (*n*=0-6) clusters. For

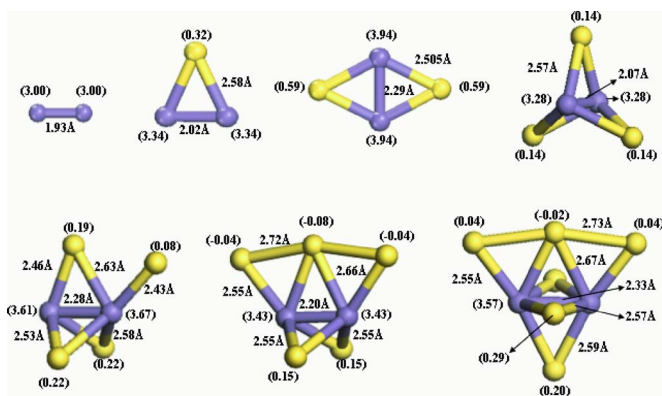


FIG. 2. (Color online) Geometry of Fe₂Au_{*n*} (*n*=0-6) clusters. The numbers in parentheses are magnetic moments (in μ_B) located on Fe and Au atoms.

Fe₂, the equilibrium bond length is 1.93 Å, and each Fe atom carries the magnetic moment of 3.0 μ_B .

When one Au atom is absorbed, the Fe-Fe bond length is elongated to 2.02 Å, and accordingly the moment increased to 3.34 μ_B . The Au atom is ferromagnetically polarized with a moment of 0.32 μ_B . When the second Au atom is added, the Fe-Fe bond length is increased further to 2.29 Å, and the moment on Fe atom becomes 3.94 μ_B . However, when the third Au atom is added, Fe₂ molecule becomes more compact with the bond length of 2.07 Å and the moment decreases to 3.28 μ_B . The fourth Au atom is on the top site of one Fe atom which stretches the Fe-Fe bond length to 2.28 Å. In this case, two Fe atoms are no longer equivalent, and the average moment of Fe is 3.64 μ_B . Up to now, all the Au atoms are ferromagnetically polarized with respect to the orientation of magnetic moment on Fe atoms. This situation is changed when the fifth Au atom is introduced, where three Au atoms form a chain with a negative moment, while the other two Au atoms are separately bonded to Fe, with a positive moment.

The Fe-Fe bond length has decreased marginally to 2.20 Å resulting in a moment of 3.43 μ_B . When the sixth Au atom is added, it elongates the Fe-Fe bond length to 2.33 Å and increases the Fe moment to 3.57 μ_B . It is interesting to note here that unlike in the case of Fe₂Au₅, there is only one Au atom that carries a negative moment. With 18 Au atoms absorbed, Fe₂ molecule is completely wrapped inside the gold shell. Figure 3 gives the geometry of Fe₂@Au₁₈ with C_{2v} symmetry.

The bond length between Fe atoms and the moment on Fe are 2.57 Å and 3.1 μ_B , respectively. Therefore, sequential gold coating of Fe₂ can tune the bond length as well as the moment. A summary of the effect of gold coating on Fe-Fe bond length and Fe moment is given in Fig. 4. Generally, a magnetic moment depends on two competitive basic factors: bond length and coordination number. Larger bond length favors a larger moment, whereas increasing the coordination

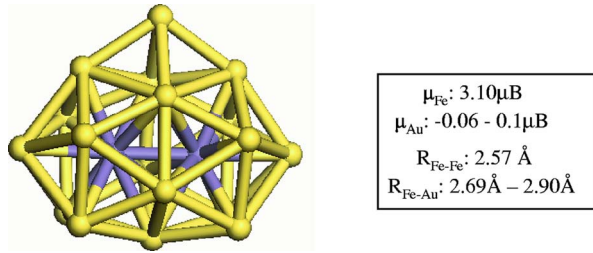


FIG. 3. (Color online) Geometry of $\text{Fe}_2\text{Au}_{18}$ with C_{2v} symmetry.

of the atom would reduce its moment. In Fe_2Au_n , for n up to 6, bond length dominates the magnetism, namely, the larger the bond length, the bigger the moment. When $n=18$, the coordination number dominates the magnetism. In this case, Fe-Fe bond length reaches 2.57 \AA , the largest one for all the cases studied, but the moment on Fe atom is only 3.1 μ_{B} , which is comparable to the value of 3.28 μ_{B} in Fe_2Au_3 with the bond length of 2.07 \AA . Thus, we conclude that the coupling between the Fe atoms remain ferromagnetic independent of the amount of gold and the moment on the Fe atom is still larger than in the bulk.

C. Magnetic coupling in a Fe core coated with Au: $\text{Fe}_{13}@Au_{42}$ and $\text{Fe}_{13}@Au_{134}$

To examine if a Fe core would also remain magnetic when wrapped in gold, we consider the Fe_{13} cluster since it has been synthesized using laser vaporization source and found to exhibit much higher intensity in time-of-flight (TOF) mass spectra than its neighbors.²⁷ The reactivity and catalysis of Fe_{13} cluster has also been studied extensively.^{21,28} Our calculations show that the optimized geometry of Fe_{13} is a distorted icosahedron, where the average bond length between the central Fe atom and the surface atom is 2.512 \AA . The average moments on the central and surface Fe atoms are 2.32 and 3.0 μ_{B} , respectively. Now we explore the changes in the geometry and moment of Fe_{13} when it is coated with gold. First, we discuss $\text{Fe}_{13}@Au_{42}$. We studied three isomers of this complex. The optimized

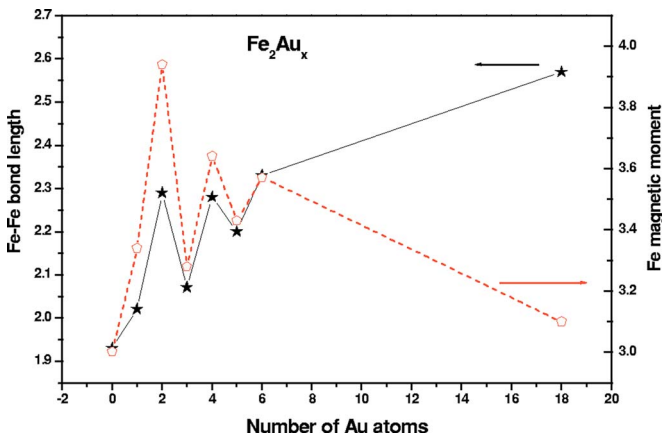


FIG. 4. (Color online) Changes of Fe-Fe bond length (in \AA , left axis) and magnetic moment located on Fe atom (in μ_{B} , right axis).

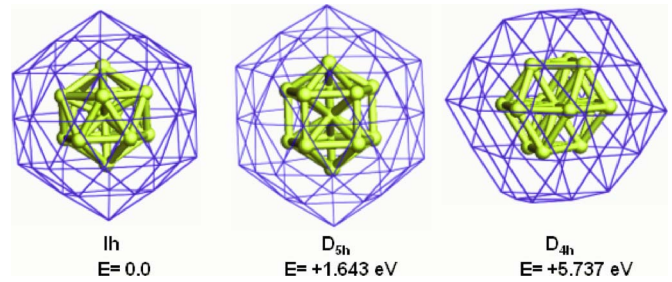


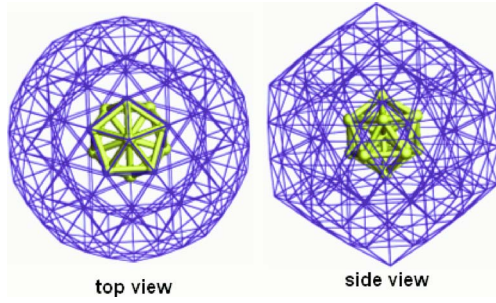
FIG. 5. (Color online) Optimized $\text{Fe}_{13}@Au_{42}$ isomers with different symmetry as shown. The relative energy E , with respect to the I_h structure is also shown.

geometries of these isomers are shown in Figure 5, whose initial geometries were icosahedron, decahedron, and octahedron, respectively. The lowest energy structure of $\text{Fe}_{13}@Au_{42}$ is an icosahedron with I_h symmetry. It is noteworthy here that while the bare Fe_{13} is a distorted icosahedron, gold coating of Fe_{13} has resulted in a perfect I_h symmetric structure. This observation is in agreement with the experimental findings that Fe-Au particles display icosahedral structure.²⁹

In the D_{5h} isomer, the Fe_{13} core is a decahedron while the Au shell becomes an icosahedron cage. In the D_{4h} isomer, both Fe_{13} core and Au shell are distorted from the initial octahedral structures. In the ground state geometry of the I_h structure, compared to the bare Fe_{13} cluster, the bond length of the Fe_{13} core is expanded by 3.2% after gold coating. While the magnetic moment of the central Fe atom increased to 2.384 μ_{B} , the moment of the outer Fe atoms is reduced to 2.923 μ_{B} from 3.0 μ_{B} due to the interactions with the gold shell. Fe-Au bond length is found to be 2.83 \AA , comparable to the values of 2.69–2.90 \AA found in $\text{Fe}_2@Au_{18}$, as we discussed above. For the gold-coating shell of Au_{42} , there are two subshells composed of (30, 12) atoms, the corresponding induced moment in these two subshells are 0.018 and 0.014 μ_{B} , respectively.

From the studies of $\text{Fe}_2@Au_{18}$ and $\text{Fe}_{13}@Au_{42}$, we can see that the large magnetic moment of Fe are more or less preserved after being coated completely with a single shell of gold atoms. To see if increasing the thickness of gold coating can retain the large magnetic moment of the iron core, we added another shell of 92 gold atoms to the $\text{Fe}_{13}@Au_{42}$ cluster resulting in $\text{Fe}_{13}@Au_{134}$ having icosahedral symmetry. The coating consists of five subshells (30, 12, 20, 60, and 12). Figure 6 shows the optimized geometry constrained to having the I_h symmetry. The addition of extra gold layers onto the $\text{Fe}_{13}@Au_{42}$ was found to have negligible effect on the bond length and the magnetic moments of the Fe_{13} core. For example, the distance from the central Fe atom to the outer Fe atom becomes 2.438 \AA and the core-shell distance becomes 2.820 \AA which are quite close to the values of 2.467 and 2.830 \AA , respectively, in $\text{Fe}_{13}@Au_{42}$. Due to the extra gold layers, the moment on the central Fe atom changes from 2.384 μ_{B} to 2.357 μ_{B} , while the moment on the Fe atom on the outer shell changes from 2.932 μ_{B} to 2.801 μ_{B} . The induced magnetic moments in the five subshells of gold are 0.015, 0.012, 0.010, 0.007, and 0.003 μ_{B} , respectively.

In Table II, we summarize the main results for Fe_{13} , $\text{Fe}_{13}@Au_{42}$, and $\text{Fe}_{13}@Au_{134}$ clusters. For a thickly coated

FIG. 6. (Color online) Optimized geometry of $\text{Fe}_{13}@Au_{134}$.

shell, it is clear that the induced moment on gold shells is mainly on the interface layers, and there are no moments on the outermost layers. Hence, this core-shell complex looks like {ferromagnetic Fe core+weakly polarized Au layers +nonmagnetic Au layers}. Therefore, the thickness of the gold shell has some effect only on the induced moment distribution in the gold shells but has little effect on the magnetic moment of the Fe core, whose large magnetic moment is very well retained. This is a very desirable property in magnetic drug delivery and hyperthermia treatment.

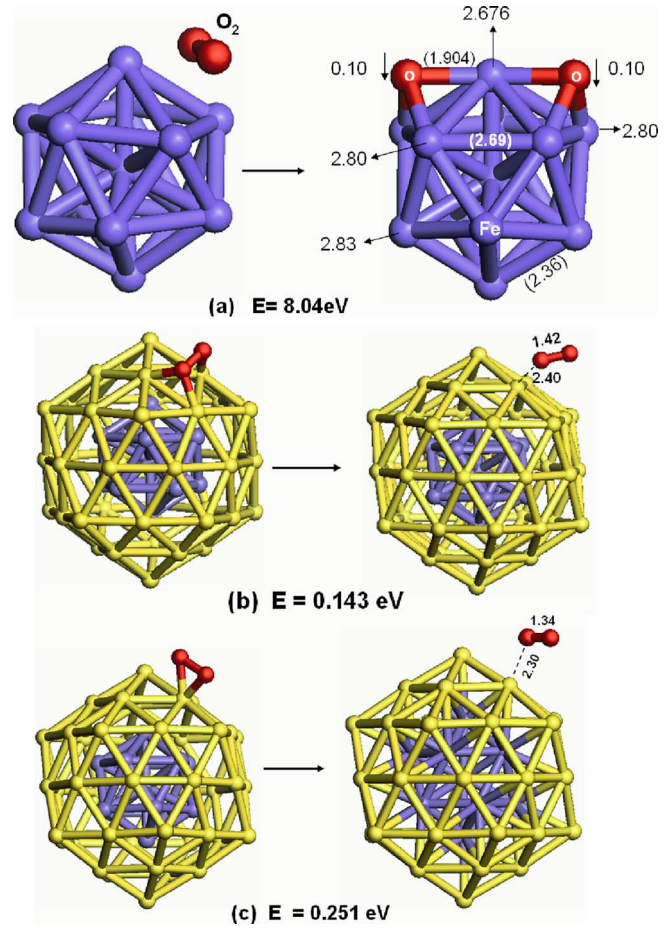
D. Oxidation of Fe_{13} and $\text{Fe}_{13}@Au_{42}$ clusters

It is well known that iron oxidizes easily and this oxidation adversely affects its magnetic properties. For example, Fe_{13} cluster reacts with oxygen forming stable Fe_{13}O_8 cluster,²¹ which greatly reduces the magnetic moment as compared to Fe_{13} . To gain a fundamental understanding of this process, we have reacted Fe_{13} and $\text{Fe}_{13}@Au_{42}$ cluster with an oxygen molecule.

We first discuss the interaction of O_2 with Fe_{13} . The starting and optimized geometries of Fe_{13}O_2 are given in Fig. 7(a). Note that O_2 dissociates and binds with the surface Fe atoms strongly with a binding energy of 8.04 eV. The total magnetic moment of Fe_{13}O_2 is $38 \mu_B$, which is reduced by $4 \mu_B$ as compared to the magnetic moment of Fe_{13} . The study of the possible absorption sites of O_2 on $\text{Fe}_{13}@Au_{42}$ is difficult as there are 12 vertices and 30 bridge sites to consider. However, the knowledge of the electronic structure of

TABLE II. Bond length (in Å) and magnetic moment (in μ_B) for $\text{Fe}_{13}@Au_n$.

	Fe_{13}	$\text{Fe}_{13}@Au_{30}@Au_{12}$	$\text{Fe}_{13}@Au_{30}@Au_{12}@Au_{60}@Au_{12}$
μ_{Fe1}	2.32	2.384	2.357
μ_{Fe2}	3.00	2.923	2.801
μ_{Au}		0.018 (1st shell) 0.014 (2nd shell)	0.015 (1st shell) 0.012 (2nd shell) 0.010 (3rd shell) 0.007 (4th shell) 0.003 (5th shell)
R_{Fe1}	2.390	2.457	2.438
R_{Fe2}	2.512	2.594	2.543
$R_{\text{Fe-Au}}$		2.830	2.820

FIG. 7. (Color online) Initial and optimized geometries for $\text{Fe}_{13}\text{-O}_2$ and $\text{Fe}_{13}@Au_{42}\text{-O}_2$. The bond length (in Å, the numbers in parentheses) and moment (in μ_B) are given for $\text{Fe}_{13}\text{-O}_2$. The bond length of O_2 and the distance between O_2 and Au shell are shown in (b) and (c).

$\text{Fe}_{13}@Au_{42}$ helps. The coating of Fe_{13} by Au allows charges to be transferred from Fe_{13} core to the coating shell. This is because Au is the most electronegative metal, comparable to selenium, and is only slightly more electropositive than sulfur and iodine. Therefore, it can form ionic compounds such as Au^-Cs^+ .³⁰ Similar charge transfer was also found in the gold-coated SiO_2 system.⁵ We found that in $\text{Fe}_{13}@Au_{42}$, the transferred charges are primarily accumulated on the bridge sites. Therefore these bridge sites are expected to be the preferred absorption sites for O_2 .²²

We have tried two different initial absorption configurations as shown in Figs. 7(b) and 7(c). In both cases, O_2 interacts weakly with $\text{Fe}_{13}@Au_{42}$. The interaction energies are 0.143 eV and 0.251 eV and the distances between the Au and O atom are respectively 2.4 and 2.3 Å. This is in agreement with experiments^{12,14} where nanoparticles coated with Au have been found to be resistant to corrosion.

IV. DISCUSSIONS AND SUMMARY

Although gold-coated Fe particles, usually studied in experiments, have a diameter of about 10 nm, the clusters we

have studied here, namely, $\text{Fe}_{13}@\text{Au}_{42}$ and $\text{Fe}_{13}@\text{Au}_{134}$, have diameters of 1.036 and 1.626 nm, respectively. There are two main reasons why we used these small systems: (1) Smaller size particles may have an advantage in penetrating the crowded environments such as biological milieu of cells and live tissues and can be more effective for drug delivery. In fact, there are some regions in the human body (e.g., inside kidney tubules and those beyond the blood brain barrier) that have special types of cell to cell contacts called the zonulae occludentes, which are about 1 nm wide. (2) Small size allows us to do accurate calculations. It would be ideal if one could carry out a calculation on a 10 nm size gold-coated iron nano nanoparticles using the same level of theory as used here; however, such a calculation is beyond the scope of present computer power. Our systematic studies on the small size clusters, however, allow us to draw some general conclusions that are valid for larger particles: (1) The magnetic moment of a Fe atom is enhanced over bulk value and

remains insensitive to the amount of gold coating. (2) The coupling between the Fe atoms remains ferromagnetic irrespective of the number of gold layers. (3) The iron core remains magnetic with a large magnetic moment. (4) Coating of gold also prevents iron from oxidation and may also prevent their coalescence and formation of thromboses in the body. (5) Gold coating improves the biocompatibility and provides a platform for magnetic particles to be functionalized.

ACKNOWLEDGMENTS

The authors thank the crew of the Center for Computational Materials Science, the Institute for Materials Research, Tohoku University (Japan), for their continuous support of the HITACH SR8000 supercomputing facility. Q. Sun thanks M. Hajaligol, B. Reddy, C. Gonzalez, and V. Mujica for stimulating discussions.

*Corresponding author. Electronic address: qsun@vcu.edu

¹S. Mornet, S. Vasseur, F. Grasset, and E. Duguet, *J. Mater. Chem.* **14**, 2161 (2004).

²P. Tartaj, M. Morales, S. V. Verdager, T. G. Carreño, and C. J. Serna, *J. Phys. D* **36**, R182 (2003).

³Q. A. Pankhurst, J. Connolly, S. K. Jones, and J. Dobson, *J. Phys. D* **36**, R167 (2003).

⁴R. F. Service, *Nature (London)* **306**, 2035 (2004).

⁵Q. Sun, Q. Wang, B. K. Rao, and P. Jena, *Phys. Rev. Lett.* **93**, 186803 (2004).

⁶J. Aizpurua, P. Hanarp, D. S. Sutherland, M. Käll, G. W. Bryant, and F. J. García de Abajo, *Phys. Rev. Lett.* **90**, 057401 (2003).

⁷Q. Sun, Q. Wang, P. Jena, R. Note, J. Z. Yu, and Y. Kawazoe, *Phys. Rev. B* **70**, 245411 (2004).

⁸M. P. Johansson, D. Sundholm, and J. Vaara, *Angew. Chem., Int. Ed.* **43**, 2678 (2004).

⁹Y. Kondo and K. Takayanagi, *Science* **289**, 606 (2000).

¹⁰W. L. Zhou, E. E. Carpenter, J. Lin, A. Kumbhar, J. Sims, and C. J. O'Connor, *Eur. Phys. J. D* **16**, 289 (2001).

¹¹E. E. Carpenter, *J. Magn. Magn. Mater.* **225**, 17 (2001).

¹²J. Lin, W. Zhou, A. Kumbhar, J. Wiemann, J. Fang, E. E. Carpenter, and C. J. O'Connor, *J. Solid State Chem.* **159**, 26 (2001).

¹³S.-J. Cho, J.-C. Idrobo, J. Olamit, K. Liu, N. D. Browning, and S. M. Kauzlarich, *Chem. Mater.* **17**, 3181 (2005).

¹⁴M. Chen, S. Yamamuro, D. Farrell, and S. A. Majetich, *J. Appl. Phys.* **93**, 7551 (2003).

¹⁵J. Guevara, A. M. Llois, and M. Weissmann, *Phys. Rev. Lett.* **81**, 5306 (1998).

¹⁶Q. Wang, Q. Sun, J. Z. Yu, Y. Hashi, and Y. Kawazoe, *Phys. Lett. A* **267**, 394 (2000).

¹⁷M. J. Frischl *et al.*, GAUSSIAN03 (Gaussian, Pittsburgh, 2003).

¹⁸G. Kresse and J. Furthmüller, *Phys. Rev. B* **54**, 11169 (1996).

¹⁹A. D. Becke, *Phys. Rev. A* **38**, 3098 (1988).

²⁰J. P. Perdew and Y. Wang, *Phys. Rev. B* **45**, 13244 (1992).

²¹Q. Wang, Q. Sun, M. Sakurai, J. Z. Yu, B. L. Gu, K. Sumiyama, and Y. Kawazoe, *Phys. Rev. B* **59**, 12672 (1999).

²²Q. Sun, P. Jena, Y. D. Kim, M. Fischer, and G. Gantefor, *J. Chem. Phys.* **120**, 6510 (2004).

²³Q. Sun, Q. Wang, Y. Kawazoe, and P. Jena, *Eur. Phys. J. D* **29**, 231 (2004).

²⁴S. Khmelevskiy, J. Kudrnovsky, B. L. Gyorffy, P. Mohn, V. Drchal, and P. Weinberger, *Phys. Rev. B* **70**, 224432 (2004).

²⁵C. M. Fang, R. A. de Groot, M. M. J. Bischoff, and H. van Kempen, *Phys. Rev. B* **58**, 6772 (1998).

²⁶J. Wang, Z. Li, Q. Sun, and Y. Kawazoe, *J. Magn. Magn. Mater.* **183**, 42 (1998).

²⁷M. Sakurai, K. Watanabe, K. Sumiyama, and K. Suzuki, *J. Chem. Phys.* **111**, 235 (1999).

²⁸F. Huisken, B. Kohn, R. Alexandrescu, and I. Morjan, *J. Chem. Phys.* **113**, 6579 (2000).

²⁹D. K. Saha, K. Koga, and H. Takeob, *Eur. Phys. J. D* **9**, 539 (1999).

³⁰G. C. Bond, *Catal. Today* **72**, 5 (2002).